Outward Transport of High-Temperature Materials Around the Midplane of the Solar Nebula
Fred J. Ciesla, *et al.*
Science **318**, 613 (2007);
DOI: 10.1126/science.1147273

Outward Transport of High-Temperature Materials Around the Midplane of the Solar Nebula

Fred J. Ciesla

The Stardust samples collected from Comet 81P/Wild 2 indicate that large-scale mixing occurred in the solar nebula, carrying materials from the hot inner regions to cooler environments far from the Sun. Similar transport has been inferred from telescopic observations of protoplanetary disks around young stars. Models for protoplanetary disks, however, have difficulty explaining the observed levels of transport. Here I report the results of a new two-dimensional model that shows that outward transport of high-temperature materials in protoplanetary disks is a natural outcome of disk formation and evolution. This outward transport occurs around the midplane of the disk.

Observations of molecular clouds, the material from which planetary systems form, indicate that the silicates contained within are predominantly amorphous (*1*)—their atoms are randomly oriented with respect to one another. Thus, it is surprising that comets contain abundant crystalline silicates—grains whose atoms are arranged in ordered, repeating patterns (*2*, *3*). Because crystalline grains can form from amorphous precursors through processing at high temperatures (>1100 K) (*2*, *4*), it was suggested that these silicates originated in the hot, inner regions of the solar nebula and were transported outward beyond 15 to 20 astronomical units (AU), where long-period comets formed (*2*). This hypothesis is supported by the findings of the Stardust mission (*5*, *6*). Not only do the samples collected from Comet Wild 2 contain large amounts of crystalline Mg-rich olivine, but a refractory grain dubbed "Inti" has also been identified. This grain has mineralogy and oxygen isotope ratios similar to those of the calcium- and aluminum-rich inclusions (CAIs) found in chondritic meteorites, suggesting a common origin (*7*). CAIs record temperatures >1500 K and likely formed close to the Sun (*8*). Spectral signatures of crystalline grains in the cool, outer regions of disks around other stars (*9*, *10*) indicate that outward transport of high-temperature materials is a fundamental consequence of protoplanetary disk evolution.

Protoplanetary disks evolve as they drive mass inward to be accreted by their central stars (*11*). The mechanism responsible for this evolution is not well understood, but one popular hypothesis is that the transport arises due to a turbulent viscosity given by $\alpha c^2/\Omega$, where c is the local speed of sound, Ω is the local Keplerian angular frequency, and α is a parameter, <1, that characterizes the level of turbulence (*12*). The viscosity may be due to a process like the magnetorotational instability (MRI) (*13*), and when coupled with the differential rotation rates of a disk, generates shear stresses between neighboring parcels of gas. While these stresses drive mass inward, the turbulence allows materials to diffuse outwards. Numerical investigations (*3*, *14*) found that delivering crystalline grains to the comet-formation region in this manner is inefficient, because the inward flows associated with disk evolution frustrate the outward diffusion of particles. To deliver processed grains at high abundances (>10%) to the comet-formation region, the transport distance had to be small (a few AU). This meant that temperatures in the solar nebula had to exceed 1000 K out to 10 AU, which requires mass accretion rates ~10^{-5} solar masses ($M_\odot$)/year (*3*). However, this value implies a short lifetime for the solar nebula, because a negligible fraction of its mass would remain after 10^6 years. This is inconsistent with the age differences between CAIs and chondrules in chondritic meteorites (*15*) and models of Jupiter's formation by core accretion (*16*), both of which indicate that the solar nebula retained a substantial amount of mass for >2 million years. Formation of the giant planets by disk fragmentation (*17*) is also problematic because these disks would be too hot to be gravitationally unstable.

These numerical studies used one-dimensional (1D) models for the solar nebula that tracked how the surface density of grains evolved due to the effects of diffusion, gas drag, and viscous flows. In these models, the motions due to gas drag and viscous flows are found by determining the characteristic (midplane) and net (vertically averaged) velocities, respectively, and applying them to all particles at a given radial distance from the Sun (*3*, *14*, *18*). In reality, the dynamics of solid particles in the solar nebula depended strongly on the values of the local gas volume density and pressure, as well as their respective gradients (*19*), all of which varied with height above the nebular midplane (Fig. 1). A major consequence of these variations is that the viscous stresses that developed within the nebula also varied with height, producing rapid inward flows along the surfaces (high altitudes) of the disk (*20*–*22*). The flow rates fell off at lower altitudes and, indeed, were directed outward around the midplane (Fig. 2).

To account for these effects, I have modeled particle transport in a viscous, two-dimensional (2D) protoplanetary disk. The model tracks the radial and vertical transport of solids due to diffusion, viscous flows, gas drag, and settling due to gravity (*23*). The 2D model reveals that outward transport in a viscous disk is much more efficient than found by 1D studies (Fig. 3). This increased efficiency is due largely to the ease with which particles are transported outward around the midplane, the reasons for which are twofold. First, outward diffusion of materials occurs more rapidly in regions of the disk that have negative density gradients. Second, particles that diffuse outward in this region do so without having to battle inward flows associated

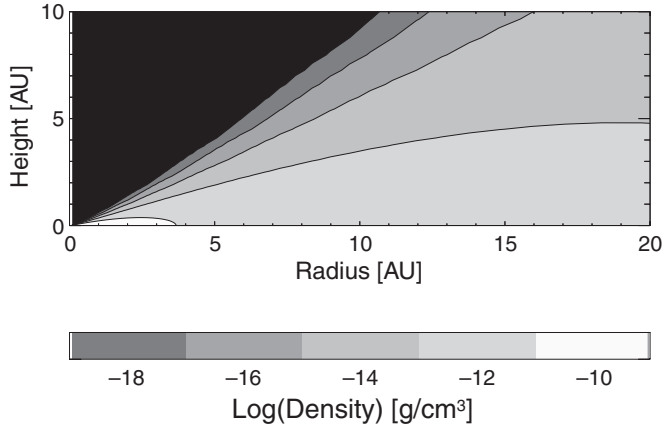

Fig. 1. Gas volume density contours for a disk in hydrostatic equilibrium whose surface density is given by $\Sigma(r) = 6300\ r_{AU}^{-1}$ g/cm^2 and temperature structure by $T(r) = 1500\ r_{AU}^{-0.5}$ K, where r_{AU} is the radial distance in astronomical units (AU). This corresponds to a disk with a mass accretion rate of $5 \times 10^{-7}\ M_\odot$/year (for $\alpha = 0.002$), which is typical for young T-Tauri stars (*11*, *12*). The disk thickness ($H = c/\Omega$) increases with distance from the star as the vertical component of gravity decreases. Thus, the gas density monotonically decreases with distance around the midplane of the disk, but increases with radial distances for extended regions at higher altitudes. The pressure contours behave similarly.

Department of Terrestrial Magnetism, Carnegie Institution of Washington, 5241 Broad Branch Road, NW, Washington, DC 20015, USA. E-mail: fciesla@ciw.edu

with disk evolution—indeed, their outward transport may be further encouraged by the outward flows that are present. Those materials that diffuse vertically out of this region are pushed back toward the star as outward diffusion slows and the viscous flows are directed inward.

Thus, the level to which high-temperature materials can be delivered to the cool, outer regions of a protoplanetary disk is controlled by their residence time in the "outward transport region" (OTR) around the midplane. Long residence times in the OTR can be achieved in two ways. The first is if the OTR occupies large volumes within the disk, a condition that is determined by the disk structure (Fig. 2). Disks with relatively steep surface density gradients will have larger OTRs because they have less mass in the outer disk to drive inward flows through viscous stresses. As a result, these flows are relegated to the uppermost layers of the disk where the radial volume density gradients start to become positive. This allows larger levels of outward transport (Fig. 3). Conversely, a disk with a more shallow surface density profile has a smaller OTR, resulting in less outward transport and limiting the materials in the outer disks to amorphous grains left over from the parent molecular cloud. Molecular cloud collapse calculations (*24*) predict that disks will develop surface density profiles that initially vary as $r^{-1.5}$; however, deviations from this profile arise due to nonsymmetry and magnetic-field effects, and therefore disks with a range of structures are expected. Because the largely molecular hydrogen gas in protoplanetary disks cannot be directly observed, the results here suggest that the crystallinity fraction and distribution in these disks can be used as a diagnostic of the disk structure and, when combined with other observations such as the opacity variations across the disk, may help untangle the physical properties of the disk.

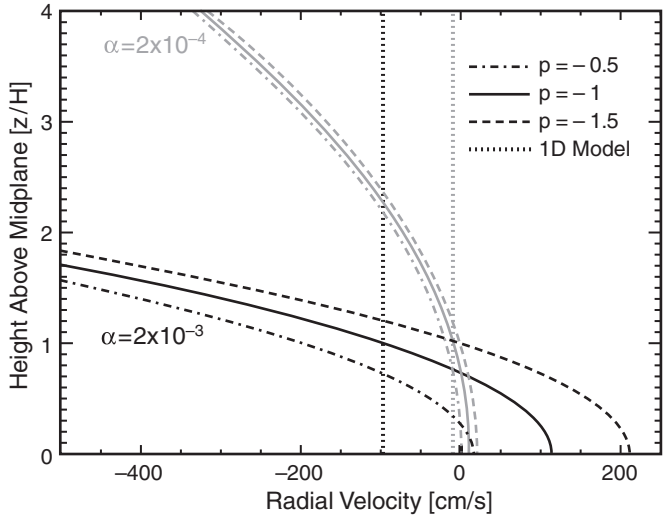

Fig. 2. The radial velocity of the gas at 1 AU in viscous accretion disks with different viscosities (values of α) and different surface density radial dependences (r_{AU}^{p}). The thermal structure is the same as in Fig. 1. The flows are determined largely by the radial gradients in gas density and temperature (*20*–*22*); thus, vertical variations in temperature would not produce substantially different results from those shown. The 1D steady-state advective velocities are shown for comparison.

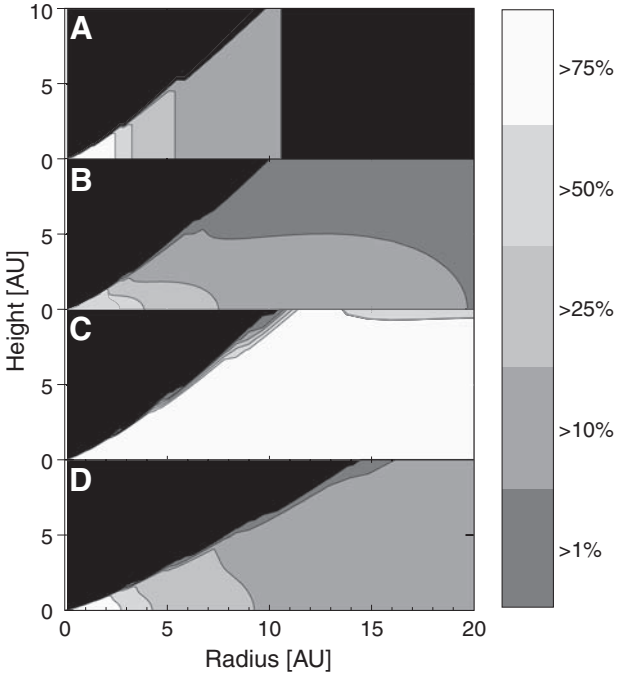

Fig. 3. Contour plots for the silicate crystallinity fraction in steady-state protoplanetary disks. In (**A**) and (**B**), the disk has the same structure and evolves as described in Fig. 1. (A) shows the results of a 1D model (*23*), whereas (B) uses the 2D model developed here. Silicates are assumed to be 1-μm spheres and initially distributed in the disk at a crystallinity fraction of 1%. Grains that are exposed to temperatures above 1100 K become crystalline, because the annealing time (<10 min) is negligible when compared to all other time scales considered (*2*, *4*). In (**C**), the disk surface density falls off as $r^{-1.5}$ with all other disk properties kept the same. In (**D**), the same disk as in (A) and (B) is used, except that solids are contained in millimeter-sized aggregates. In all cases, the vertical distribution of solids is characterized by a thickness, $H_d = [\alpha/(1 + St)]^{0.5} H$ (*19*).

Alternatively, long residence times in the OTR can be attained if materials are contained in large grains or were incorporated into larger aggregates through collisions and sticking with other grains (*25*). These larger objects would not diffuse vertically as efficiently as smaller particles (*19*), leading to higher concentrations in the OTR and larger outward fluxes (Fig. 3). If high-temperature materials were delivered in larger assemblages, these aggregates and grains would be susceptible to disruption from the energetic collisions that arise in turbulent environments (*25*). Such collisions would thus populate the outer disk with high-temperature fine-grained materials whose spectral signatures could then be observed (*9*, *10*).

That outward transport occurs most efficiently around the midplane of the disk suggests that the fraction of crystalline grains in a disk will correlate with the amount of settling that occurs, which increases as solids grow. These correlations are indeed observed because those disks that are inferred to have large crystallinity fractions based on the observed spectra are best fit by models in which the solid subdisk is flat, rather than flared (*10*). Such correlations are counter to the 1D model predictions, where an increase in particle size leads to a decrease in the outward transport efficiency because larger particles diffuse less efficiently and migrate inward more rapidly due to gas drag (*19*). Here, the outward flows within the OTR counteract the inward motions due to gas drag. These flows could also preserve the 0.1- to 1-cm CAIs in the solar nebula for the millions of years between their formation and their incorporation into meteorite parent bodies (*15*, *18*).

The variations in radial transport dynamics with height produce vertical gradients in the abundance of crystalline grains in the disk (Fig. 3). Thus, infrared observations of protoplanetary disks, which only detect radiation from the disk surfaces, will lead to underestimates of the fraction of material that was processed at high temperatures. Therefore, the reported crystallinity fractions for protoplanetary disks (*9*, *10*) should be taken as lower bounds. Such gradients are not predicted in 1D models because of the implicit assumption that all materials are well mixed with height.

This work shows that outward transport of high-temperature materials naturally occurs around the midplane of turbulent protoplanetary disks. This mode of transport would take place even if layered accretion (*26*) occurred—where the MRI generated a turbulent viscosity in the surface layers of the disk, leaving the midplane surrounded by a "Dead Zone." Hydrodynamic effects can produce turbulence even in cold,

neutral parts of a disk (*27*), allowing solids to diffuse outward around the midplane while still avoiding the inward flows that would frustrate their transport to the outer disk. The only requirement for this model is that the disk was hot enough to process materials at the needed temperatures. Although high mass accretion rates are initially needed to produce these temperatures, the rates that are needed to deliver large amounts of high-temperature materials to the outer disk are typical for young T-Tauri stars (*11*) and more than an order of magnitude less than required by previous models (*3*).

An important consequence of this model is that the thermally processed grains would have remained in contact with the nebular gas throughout their transport, allowing volatiles to condense on their surfaces in cooler environments. In the X-wind model (*28*), grains are processed by radiation from the Sun as they are launched above the disk in bipolar outflows. These grains would have lost their volatiles upon being heated, then decoupled from the gas to rain back onto the solar nebula. As these grains fell onto the solar nebula in the comet-formation region, there would be mixing between two components: the solar composition materials that were already present and the more refractory crystalline grains. Thus, comets that grew from these materials would be depleted in volatile elements, and those depletions would correlate with the amount of crystalline materials they contain. Preliminary analyses of the Stardust samples indicate that Comet Wild 2 exhibits no such depletions (*29*).

References and Notes

1. F. Kemper, W. J. Vriend, A. G. G. M. Tielens, *Astrophys. J.* **609**, 826 (2004).
2. J. A. Nuth III, H. G. M. Hill, G. Kletetschka, *Nature* **406**, 275 (2000).
3. D. Bockelée-Morvan, D. Gautier, F. Hersant, J.-M. Hure, F. Robert, *Astron. Astrophys.* **384**, 1107 (2002).
4. S. L. Hallenbeck, J. A. Nuth III, R. N. Nelson, *Astrophys. J.* **535**, 247 (2000).
5. D. Brownlee *et al.*, *Science* **314**, 1711 (2006).
6. M. E. Zolensky *et al.*, *Science* **314**, 1735 (2006).
7. K. D. McKeegan *et al.*, *Science* **314**, 1724 (2006).
8. G. J. MacPherson, D. A. Wark, J. T. Armstrong, in *Meteorites and the Early Solar System*, J. F. Kerridge, M. S. Matthews, Eds. (Univ. of Arizona Press, Tucson, 1988), pp. 746–807.
9. R. van Boekel *et al.*, *Nature* **432**, 479 (2004).
10. D. Apai *et al.*, *Science* **310**, 834 (2005).
11. L. Hartmann, N. Calvet, E. Gullbring, P. D'Alessio, *Astrophys. J.* **495**, 385 (1998).
12. J. E. Pringle, *Annu. Rev. Astron. Astrophys.* **19**, 137 (1981).
13. S. A. Balbus, J. F. Hawley, *Astrophys. J.* **376**, 214 (1991).
14. H.-P. Gail, *Astron. Astrophys.* **378**, 192 (2001).
15. Y. Amelin, A. N. Krot, I. D. Hutcheon, A. A. Ulyanov, *Science* **297**, 1678 (2002).
16. O. Hubickyj, P. Bodenheimer, J. J. Lissauer, *Icarus* **179**, 415 (2005).
17. A. P. Boss, *Science* **276**, 1836 (1997).
18. J. N. Cuzzi, S. S. Davis, A. R. Dobrovolskis, *Icarus* **127**, 290 (2003).
19. J. N. Cuzzi, S. J. Weidenschilling, in *Meteorites and the Early Solar System II*, D. S. Lauretta, H. Y. McSween Jr., Eds. (Univ. of Arizona Press, Tucson, 2006), pp. 353–381.
20. V. A. Urpin, *Sov. Astron.* **28**, 50 (1984).
21. T. Takeuchi, D. N. C. Lin, *Astrophys. J.* **581**, 1344 (2002).
22. Ch. Keller, H.-P. Gail, *Astron. Astrophys.* **415**, 1177 (2004).
23. Materials and methods are available as supporting material on *Science* Online.
24. R. Hueso, T. Guillot, *Astron. Astrophys.* **442**, 703 (2005).
25. C. P. Dullemond, C. Dominik, *Astron. Astrophys.* **434**, 971 (2005).
26. C. F. Gammie, *Astrophys. J.* **457**, 355 (1996).
27. B. Mukhopadhyay, N. Afshordi, R. Narayan, *Astrophys. J.* **629**, 383 (2005).
28. F. H. Shu, H. Shang, T. Lee, *Science* **271**, 1545 (1996).
29. G. J. Flynn *et al.*, *Science* **314**, 1731 (2006).

30. I thank J. Chambers, J. Cuzzi, and J. Nuth for suggestions that led to improvements to this manuscript. This research was supported by funds from the Carnegie Institution of Washington.

Supporting Online Material

www.sciencemag.org/cgi/content/full/318/5850/613/DC1
Materials and Methods
References

2 July 2007; accepted 25 September 2007
10.1126/science.1147273

A Surface-Tailored, Purely Electronic, Mott Metal-to-Insulator Transition

R. G. Moore,[1] Jiandi Zhang,[2,3] V. B. Nascimento,[1] R. Jin,[3] Jiandong Guo,[1] G.T. Wang,[4] Z. Fang,[4] D. Mandrus,[3] E. W. Plummer[1,3]

Mott transitions, which are metal-insulator transitions (MITs) driven by electron-electron interactions, are usually accompanied in bulk by structural phase transitions. In the layered perovskite $Ca_{1.9}Sr_{0.1}RuO_4$, such a first-order Mott MIT occurs in the bulk at a temperature of 154 kelvin on cooling. In contrast, at the surface, an unusual inherent Mott MIT is observed at 130 kelvin, also on cooling but without a simultaneous lattice distortion. The broken translational symmetry at the surface causes a compressional stress that results in a 150% increase in the buckling of the Ca/Sr-O surface plane as compared to the bulk. The Ca/Sr ions are pulled toward the bulk, which stabilizes a phase more amenable to a Mott insulator ground state than does the bulk structure and also energetically prohibits the structural transition that accompanies the bulk MIT.

The insulating phase associated with metal-insulator transitions (MITs) (*1*–*4*) can be described as either a band insulator (such as silicon) or a Mott insulator (such as nickel oxide). A band insulator has an even number of electrons per unit cell that can be described adequately by an independent electron theory, where all of the bands are either filled or empty at 0 K. If the number of electrons in the unit cell is odd, then band theory always predicts metallicity, but when the onsite Coulomb interaction (U) is comparable in magnitude to the bandwidth (W), the material can become a Mott insulator (*1*, *2*). A transition from the Mott insulating phase to the metallic phase can be induced by temperature, pressure, magnetic field, or doping (*4*). Normally, the MIT for a band insulator is accompanied by a structural phase transition that changes or breaks the symmetry (*5*, *6*). The simplest example is a one-dimensional chain of atoms, which, as Peierls showed (*3*), is unstable because of the degeneracy caused by Fermi surface nesting at 2 k_F, where k_F is the Fermi wavevector. The lattice reconstructs itself, doubling the periodicity and lowering the electronic energy by creating a gap at the Fermi energy (E_F).

In contrast, an inherent Mott transition should be purely electronic in origin and not assisted by a structural transition (*1*, *2*, *5*). In practice, almost all of the highly correlated materials with a large enough ratio of U/W to be Mott insulators exhibit close coupling between charge, spin, and lattice, so that the Mott transition is nearly always accompanied by a structure transition. This situation complicates the understanding of the basic mechanism of a Mott MIT as a transition driven by the electron-electron (*e-e*) correlations. We now show that the surface layer of a Mott insulator can display a MIT independent of a structural transition.

The layered ruthenate $Ca_{2-x}Sr_xRuO_4$ shows a rich array of ground states that are associated with the intricate couplings between lattice, electron, and spin degrees of freedom (*7*–*9*). Ca^{2+} replacement of Sr^{2+} gradually enhances the rotational and tilt distortion of the RuO_6 octahedra, starting with a tetragonal *I4/mmm* structure for Sr_2RuO_4, leading to an *I4*$_1$*/acd* structure for $Ca_{1.5}Sr_{0.5}RuO_4$, and ending with an orthorhombic *S-Pbca* structure for Ca_2RuO_4 (*9*). These structural changes lead to an evolution of the ground state, from an unconventional superconducting state in Sr_2RuO_4 (*10*) to a quantum critical point at $x = x_c \sim 0.5$ (where c is critical) and to an antiferromagnetic Mott insulating phase when $x < 0.2$ (*7*, *8*).

The layered structure of this material, which plays a key role in the anisotropic transport and magnetic properties (*7*, *8*), also makes the crystal

[1]Department of Physics and Astronomy, University of Tennessee, Knoxville, TN 37996, USA. [2]Department of Physics, Florida International University, Miami, FL 33199, USA. [3]Materials Science and Technology Division, Oak Ridge National Laboratory, Oak Ridge, TN 37831, USA. [4]National Laboratory for Condensed Matter Physics, Institute of Physics, Chinese Academy of Sciences, Beijing 100080, China.